

INFLUENCE OF HEAT TRANSFER DYNAMICS ON HARDNESS DISTRIBUTION AFTER QUENCHING

VPLIV DINAMIKE PRENOSA TOPLOTE NA PORAZDELITEV TRDOTE PO KALJENJU

BOŽIDAR LIŠČIĆ

Faculty of Mechanical Engineering and Naval Architecture, Ivana Lučića 5, Zagreb, Croatia

Prejem rokopisa - received: 1997-10-01; sprejem za objavo - accepted for publication: 1997-10-21

The pattern of hardness distribution on round bars' cross-section after quenching was studied in relation to the change of heat transfer on the workpiece surface. It was found that a 'delayed quenching', producing a discontinuous change of cooling rate, may result in higher hardness in the core, than at the surface. This phenomenon called 'inverse hardening' has been theoretically explained by Shimizu and Tamura. It depends on: hardenability of the steel, cross-section size of the workpiece and on quenching condition, and is related to the incubation period consumed before the cooling rate was changed. Own experiments using cylindrical specimens of 50 mm Dia, made of AISI-4140 steel, have shown that Controllable Delayed Quenching (CDQ) technology has a great potential to increase the depth of hardening, compared to conventional quenching practice. Bending fatigue tests with inverse hardened and tempered specimens have shown a significant increase of the fatigue life compared to specimens having normal hardness distribution after quenching. CDQ-technology and 'inverse hardening' can reproducibly be realized using adequate steel hardenability and cross-section size of the workpiece, by quenching in PAG polymer-solution of high concentration, or in high pressure-circulated gases.

Key words: quenching, heat transfer

Raziskane so bile značilnosti porazdelitve trdote na preseku kaljene okrogle palice v odvisnosti od spremembe prenosa toplote na površini palice. Kaljenje z zadržanjem, ki povzroča diskontinuuirno spremembo hitrosti ohlajanja, lahko ustvari večjo trdoto v jedru kot na površini. Ta pojav imenovan "inverzna utrditiv" sta teoretično razložila Shimizu in Tamura. Odvisen je od kaljivosti jekla, preseka kaljenca in od pogojev kaljenja ter je povezan z inkubacijsko dobo, ki je bila porabljena pred spremembo hitrosti ohlajanja. Naši poskusi na valjastih vzorcih ϕ 50 mm iz jekla AISI-4140 so pokazali, da ima "kontrolirano kaljenje z zadržanjem" velik potencial za povečanje globine kaljenja v primerjavi s klasičnim kaljenjem. Upogibni utrujenostni preizkusi na inverzno kaljenih in popučenih vzorcih so pokazali pomembno povečanje življenjske dobe v primerjavi z vzorci z normalno porazdelitvijo trdote po kaljenju. CDQ - tehnologija in "kaljenje z zadržanjem" sta lahko reproduktibilna, če ima jeklo primerno kaljivost in je presek kaljenca ustrezen s kaljenjem v polimerni PAG raztopini velike koncentracije ali v visokotlačni krožeči atmosferi.

Ključne besede: kaljenje, prenos toplote

1 INTRODUCTION

The practice of quenching ferrous metals has a very long history, but development of quenching technology was first of all concentrated on choosing the proper quenchant and quenching parameters, i.e. its temperature and possibly the agitation rate. Once this was fixed for a specific case, the heat transfer from the workpiece surface was governed solely by the selected quenchant and quenching parameters. Generally the idea prevailed that, for achieving a better through-hardening, a more severe quenching intensity should be applied right at the beginning of quenching. If workpieces having bigger cross-section have to be hardened through, the heat extraction from the core is the main problem. All efforts were concentrated on shortening the quenching time i.e. cooling the core of the workpiece, if possible, below M_s temperature before (according to the hardenability of the steel used) the transformation to ferrite and pearlite begins. As a result of applying a severe quenchant, high temperature gradients developed causing high thermal stresses and distortion. Using this approach two factors on which the through hardening depends, have not been taken into consideration:

a) The cooling rate in every specific point of the cross-section from the austenitizing temperature to the transformation temperature (A_1) is not critical for the microstructure and hardness after quenching. Instead the cooling rate below A_1 to the M_s point is critical, and *different points* of the cross-section pass through this temperature range (A_1 to M_s) at *different times*.

b) When severe quenching intensity is applied right from the beginning of the quenching process, the surface temperature of the workpiece is rapidly decreased to low values while the core still retains high temperature. So, when heat has to be extracted from the core, the temperature difference between surface temperature of the workpiece (T_s) and the quenchant temperature (T_0) is low and according to the Newton's law $\dot{q} = \alpha (T_s - T_0)$, the heat extracted is also low. This situation can only be improved if the heat transfer (characterized by the heat transfer coefficient α (W/m²K)) would be increased later during quenching, but this is not the case in normal quenching practice.

In 1977 the investigation published in USA by Loria¹ has shown that 'delayed quenching' can in some instances increase the depth of hardening, compared to conventional quenching practice. 'Delayed quenching'

means a relatively slow heat transfer from the workpiece surface at the beginning of quenching, followed by a fast cooling with high quenching intensity.

In the same time in Japan, Shimizu and Tamura^{2,3} have given theoretical explanation of this phenomenon stating that it is caused by *discontinuous* change in cooling rate and the incubation period (at relevant temperature) consumed, before the cooling rate was abruptly changed. Latter, experimental investigation by Liščić and Totten⁴ on one side, and numerical calculation by Chen and Zhou⁵ on the other side, have shown that at 'delayed quenching' the average cooling rate may be higher below the surface of the workpiece, than at the surface itself. While in case of normal quenching (without discontinuous change of cooling rate) the cooling rates constantly decrease from the surface towards the core, in case of 'delayed quenching' the cooling rate is lower at the surface (because of mild cooling at the beginning of the quenching process), becoming greater below the surface towards the core because of the latter abrupt change of heat transfer at the workpiece surface.

Through these works it became evident that the *heat extraction dynamics* during quenching, and not the quenching time itself is responsible for the hardness distribution on the workpiece's cross-section after quenching.

Studying the pattern of hardness distribution on round bars' cross-section after quenching Shimizu and Tamura³ have introduced the expression of 'inverse' hardening. Opposite to normal hardness distribution it shows lower hardness at the surface and higher hardness in the core.

The experiments have shown that the 'inverse' hardness distribution caused by the phenomenon of 'delayed quenching', depends on steel hardenability and on cross-section size of the workpiece. They have also shown that (in case of adequate hardenability and corresponding cross-section size) the 'delayed quenching' has a great potential to increase the depth of hardening, compared to conventional quenching practice.

Chen and Zhou⁵ state also that 'delayed quenching' can reduce residual stresses and distortion. This state of the art gives, in some instances, the possibility to achieve the biggest possible depth of hardening, simultaneously with minimum residual stress and distortion, by a Controllable Delayed Quenching.

When quenching in evaporable liquid quenchants, however, the possibility to control a preprogrammed cooling cycle and cause intentionally a 'delayed quenching' is very limited, because the only parameter that can be changed *during* the quenching process is the agitation rate.

Among all liquid quenchants only the PAG polymer-solutions possess a mechanism that enables them to realize a preprogrammed Controllable Delayed Quenching by changing the polymer concentration. The advantage of PAG solution quenchants seems to be that it is possible to achieve the proper balance of the film thickness

and film strength, depending of course on two other parameters, namely the bath temperature and the agitation rate. As it is well known higher polymer concentration gives thicker film on the workpiece surface, prolonging the vapor blanket stage i.e. causing a 'delayed quenching'.

Recently, Liščić, Grubišić and Totten⁶ have shown that bending fatigue as well as impact strength of mechanical components can be increased by 'delayed quenching'.

2 HEAT EXTRACTION DYNAMICS

It is interesting to analyse why 20 years have passed since the phenomenon of 'delayed quenching' was first published by Loria and by Shimizu and Tamura until a Controllable Delayed Quenching of real components has been investigated more in details. The answer may be found in two following reasons:

a) There was no an adequate method to test and record the quenching intensity during quenching in real practice, that could describe the heat extraction dynamics. Neither the magnetic quenchometer method, nor the cooling curve analysis of small diameter (12.5 mm Dia x 60 mm length) inconel or silver specimens can describe the heat extraction dynamics when quenching real components.

b) Only just recent investigations⁷ have revealed that polymer solutions (PAG) of higher concentration can be used as a quenchant for preprogrammed Controllable Delayed Quenching.

The newly developed Temperature Gradient Quenching Analysis System (TGQAS) using the LISCIC/NAN-MAC probe⁸ of 50 mm Dia x 200 mm length, made of AISI-304 steel, representing a real workpiece, is capable of measuring, recording and evaluation of every quenching process in workshop practice, describing the heat extraction dynamics by corresponding thermodynamic functions. The probe itself is instrumented with three thermocouples at the mid-length cross-section, measuring the temperature at the very surface, 1.5 mm below surface and in the center.

Figure 1 shows cooling curves recorded in two quenching tests: TEST-1 mineral oil of 20°C without agitation and TEST-26 PAG polymer-solution (UCONE) of 25% concentration, 40°C bath temperature and 0.8 m/s agitation rate. **Figure 2** shows calculated heat flux density vs. time between different thermocouple positions.

The characteristic feature in each of quenching tests with regard to heat extraction dynamics is the time period from the immersion up to the moment the maximum heat flux density occurs (t_{qmax}).

While for particular oil quenching (TEST-1) t_{qmax} is 14 seconds it is for the described polymer-solution quenching (TEST-26) 72 seconds. The latter one is obviously a 'delayed quenching'.

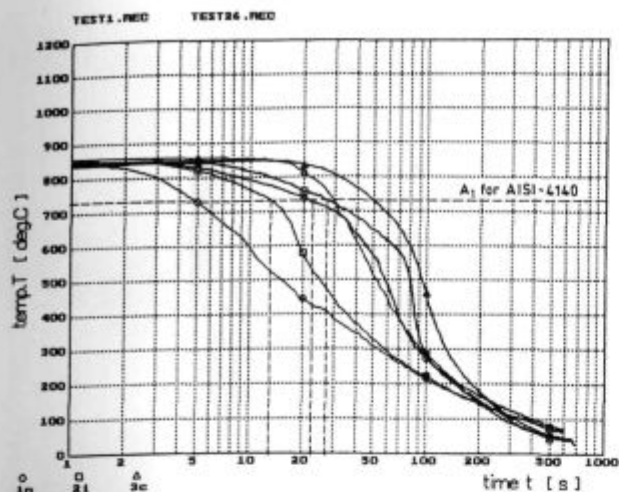


Figure 1: Two quenching tests recorded by the LISCIC/NANMAC probe (50 mm Dia x 200 mm): TEST-1 - mineral oil, 20°C, without agitation; TEST-26 - PAG polymer-solution (UCON-E), 25%, 40°C, 0.8 m/s agitation rate. Cooling curves for: surface (\square), 1.5 mm below surface (\circ) and center (Δ)

Slika 1: Dva preizkusa kaljenja registrirana z LISCIC/NANMAC preizkušancem (ϕ 50 x 200 mm). Pr. 1 - mineralno olje, 20°C, brez mešanja; Pr. 26 - PAG raztopina (UCON-E), 25%, 40°C, hitrost mešanja 0.8 m/s. Ohlajevalne krivulje za površino (\square), 1.5 mm pod površino (\circ) in središče (Δ)

quenching (TEST-26) 72 seconds. The latter one is obviously a 'delayed quenching'.

Because the heat flux density (W/m^2) is the real physical measure of the heat extraction, it is interesting to analyse and compare the heat flux density (between 1.5 mm below surface and the surface itself) v.s. time curves for both mentioned tests, shown in **Figure 2**. For particular oil quenching (TEST-1) only 12.5 seconds, right in the beginning of the quenching process, were necessary for increasing the heat flux density from a low value of 200 W/m^2 to its maximum of 2600 W/m^2 , and 35 seconds were necessary for the heat flux density to fall back to 200 W/m^2 . For particular polymer-solution quenching (TEST-26), 67 seconds or 5.4 times more were necessary for increasing the heat flux density from 200 W/m^2 to its maximum of 2250 W/m^2 , but only 23 seconds or 1.5 times less were necessary for the heat flux density to fall back to 200 W/m^2 .

This analysis clearly shows a distinct difference in heat extraction dynamics between the described oil quenching characterized by a fast cooling from the beginning, and the described polymer-solution quenching characterized by a long period of relatively slow cooling followed by a sudden change in heat extraction, after burst of the polymer film, which has caused a pronounced discontinuous change in the cooling rate, having a specific influence on transformation behavior of the steel concerned.

The discontinuous change in cooling rate, when quenching in the used polymer solution (TEST-26) can be seen in **Figure 1** as a distinct change in the slope of

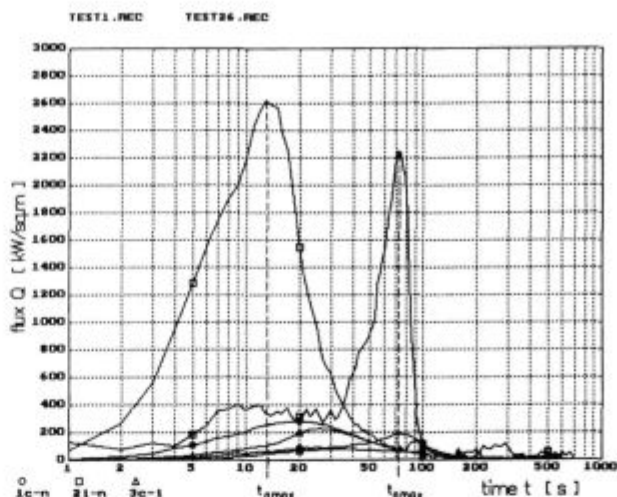


Figure 2: Heat flux densities vs. time for TEST-1 and TEST-26 calculated from recorded cooling curves. Heat flux density between 1.5 mm below surface and the surface itself (\square); between center and surface (\circ); between center and 1.5 mm below surface (Δ)

Slika 2: Gostota toplotnega toka v odvisnosti od časa za pr. 1 in 26 izračunana iz ohlajevalnih krivulj. Gostota toplotnega toka med globino 1.5 mm in površino (\square), med središče in površino (\circ) ter med središče in globino 1.5 mm (Δ)

the cooling curve for the thermocouple at 1.5 mm below surface, at 570°C.

The best way to compare the heat transfer dynamics between both described tests is to compare the amount of heat extracted at different time intervals after immersion of the probe. The curves marked with \square in **Figure 3** represent the values of the integral ($\int q dt$) below the heat

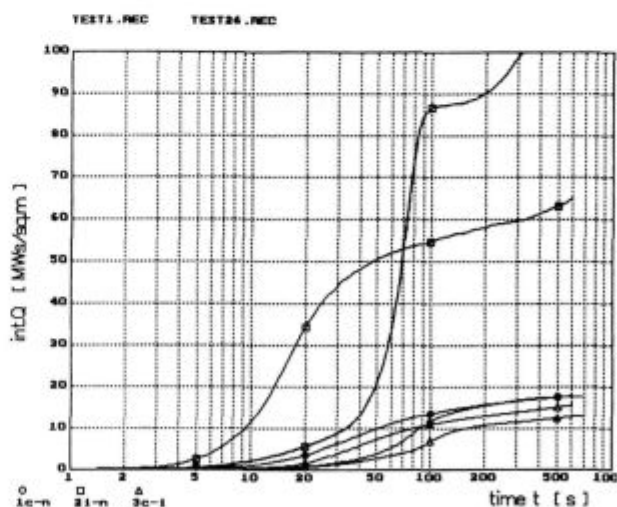


Figure 3: Integral ($\int q dt$) below heat flux density curves vs. time for TEST-1, and TEST-26, representing the amount of heat extracted. Heat extracted between 1.5 mm below surface and the surface itself (\square); between center and surface (\circ); between center and 1.5 mm below surface (Δ)

Slika 3: Integral ($\int q dt$) toplotnega toka v odvisnosti od časa za pr. 1 in 26, ki predstavlja ekstrahirano toploto. Toplota ekstrahirana med globino 1.5 mm in površino (\square), med središče in površino (\circ) ter med središče in globino 1.5 mm (Δ)

HEAT EXTRACTION DYNAMICS AT QUENCHING

The Stainless-steel Specimen of 50 mm Dia x 200 mm quenched in:
Mineral Oil of 20°C - without agitation
(wetting kinetics not included)

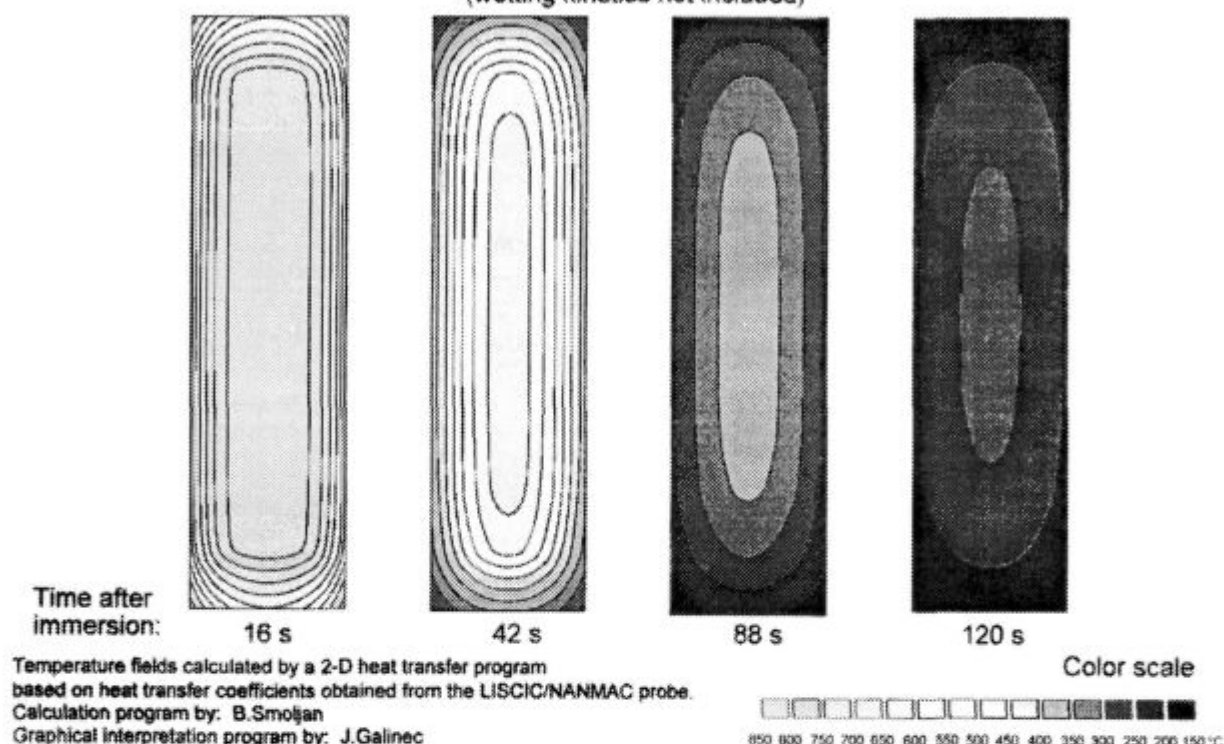


Figure 4: 2-D simulation of temperature fields when quenching the stainless steel specimen of 50 mm Dia x 200 mm in standard mineral oil of 20°C, without agitation. The calculation is based on heat transfer coefficients obtained from the LISCIC/NANMAC probe

Slika 4: 2-D simulacija temperaturnega polja med kaljenjem preizkušanca ϕ 50 x 200 mm iz nerjavnega jekla v standardnem mineralnem olju in brez mešanja. Izračunano na osnovi koeficientov prenosa toplote pridobljenih z LISCIC/NANMAC sondo

extracted (MJ/m^2), vs. time. In oil quenching (TEST-1), the amount of heat extracted starts to rise immediately in third second after immersion, reaching already after 20 seconds a value of 35 MJ/m^2 . During next 80 seconds it amounted to 55 MJ/m^2 . In the used polymer-solution quenching (TEST-26) only 5 MJ/m^2 was extracted until 20 seconds, but in next 80 seconds it reached 87 MJ/m^2 .

Using the heat transfer coefficient vs. time values calculated from the measured temperatures at the mid-length cross-section of the LISCIC/NANMAC probe, a 2-D heat transfer programme was developed for calculating temperature fields during quenching. Figure 4 shows a graphical presentation of the cooling a stainless steel specimen of 50 mm Dia x 200 mm length at: 16, 42, 88 and 120 seconds by quenching it in mineral oil of 20°C without agitation (TEST-1). Figure 5 shows the same when quenching the specimen in PAG polymer-solution (UCON-E) of 25% concentration, 40°C bath temperature and 0.8 m/s agitation rate (TEST-26). Comparison of Figure 4 and Figure 5 clearly reveals the difference in heat extraction dynamics between those two tests.

It should be emphasized that for transformation kinetics not the cooling rates from austenitizing temperature to A_1 , but the cooling rates below A_1 , are critical. For the steel grade AISI-4140 e.g. the A_1 temperature is 730°C. Analysing the average radial temperature gradients between core and surface in half length cross-section from Figure 4 and Figure 5 respectively, one gets the values given in Table I.

Table I

Austenitizing temperature: 850°C;				
Radius of specimens: 25 mm				
Time after immersion (seconds)	16	42	88	120
Average temperature gradient between core and surface in half length cross-section °C/mm	TEST-1	10	12	6
	TEST-26	2	4	10

From the calculated temperature fields in Figure 4 and Figure 5 respectively, and the values given in Table I we can derive the following:

In TEST-1 (normal case of quenching with continuous cooling rates), a cooling within the critical tempera-

HEAT EXTRACTION DYNAMICS AT QUENCHING

The Stainless-steel Specimen of 50 mm Dia x 200 mm quenched in:
PAG Polymer-solution of 25% concentration; 40°C temp.; 0.8 m/s agitation rate
(wetting kinetics not included)

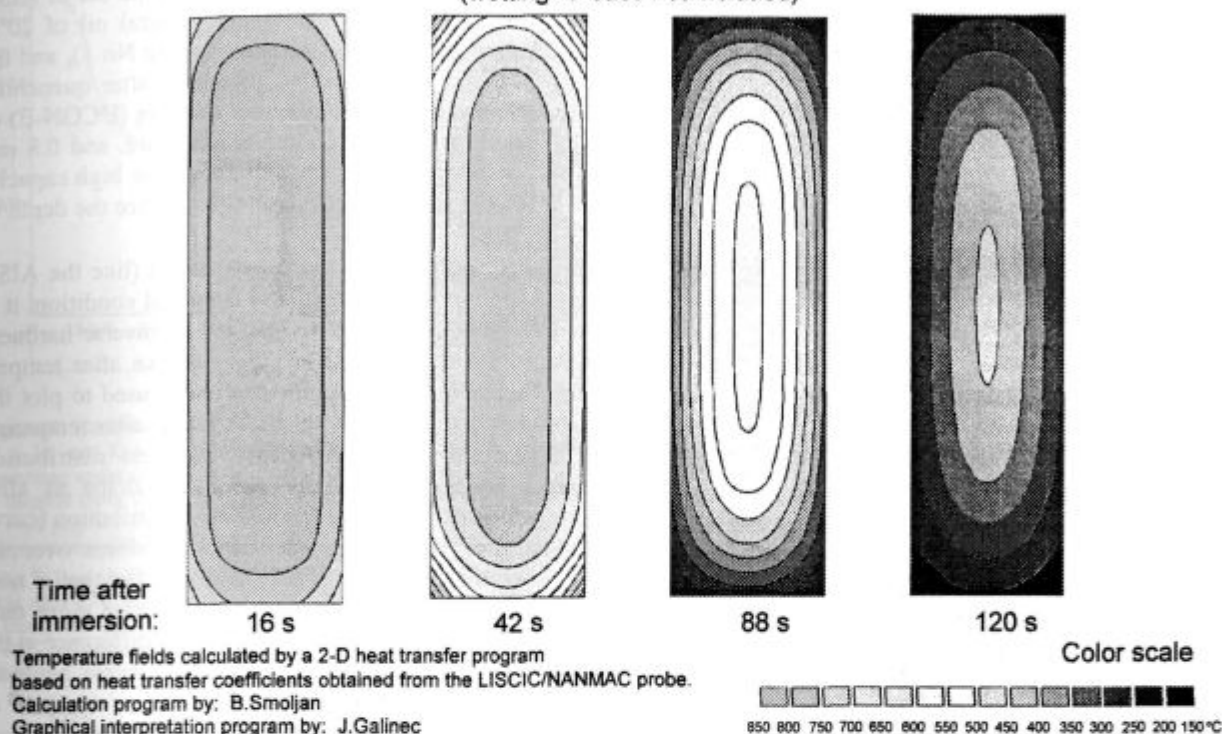


Figure 5: 2-D simulation of temperature fields by quenching the stainless steel specimen of 50 mm Dia x 200 mm in PAG polymer-solution (UCON-E) of 25% concentration; 40°C; 0.8 m/s agitation rate. The calculation is based on heat transfer coefficients obtained from the LISCIC/NANMAC probe

Slika 5: 2-D simulacija temperaturnega polja pri kaljenju preizkušanca $\phi 50 \times 200$ mm iz nerjavnega jekla v PAG polimerni raztopini (UCON-E) s koncentracijo 25%, 40°C in hitrostjo mešanja 0.8 m/s. Izračunano z uporabo koeficientov prenosa toplote pridobljenih z LISCIC/NANMAC sondo

ture range (700°C to 400°C) for the core, between 42 and 88 seconds is obtained with a decreasing temperature gradient, i.e. decreasing heat extraction flux from the core to the surface. Once the surface temperature has fallen to low values (about 200°C after 88 sec.), the heat transfer has decreased very much, because of the small temperature difference between the workpiece surface and the surrounding fluid. This heat extraction dynamics results in the normal hardness distribution i.e. substantially lower core than surface hardness.

In TEST-26 (a delayed quenching with discontinuous change of cooling rates), cooling of the core from 42 to 88 sec. (i.e. between 750°C and 600°C) is obtained with increasing temperature gradient, i.e. increasing the heat extraction flux from the core to the surface, resulting in increased core hardness.

3 TRANSFORMATION KINETICS WHEN DISCONTINUOUS CHANGE OF COOLING RATE OCCURS

From the moment the austenitized workpiece is immersed in the quenching fluid, two different processes start: the thermodynamic process of heat extraction and the metallurgical process of structure transformation. The latter one starts actually in *different times for different points* of the cross-section, when the temperature in each point falls to A_1 . These times depend on the cross-section size and the cooling intensity of the quenching fluid. The resulting hardness in a particular point depends on constituents of the structure transformed, which depend heavily on the hardenability of the steel concerned i.e. on incubation times at every isotherm. Because incubation times are counted only at temperatures below A_1 , for each particular point of the cross-section the *cooling rate in the critical temperature range A_1 to M_s is of paramount importance.*

Shimizu and Tamura² have found that the pearlitic transformation behavior with cooling rates discontinu-

ously changed during cooling was different from that given by an usual CCT diagram, and that this transformation is related to the incubation period consumed before changing the cooling rate. In case of delayed quenching some of the incubation period is consumed at the surface of the workpiece, while it is not at the center. The incubation period at any given isotherm is the time until the transformation starts (Z), while (X) is the incubation period consumed before the discontinuous change of the cooling rate has taken place. **Figure 6** which is a schematic illustration of delayed quenching, shows that at time t_1 and temperature T_1 (point P) a discontinuous change of cooling rate occurred. Up to this moment the surface of the workpiece has consumed a share (X) of the total incubation time (Z), but the center has not, because at the moment t_1 the center had a temperature above A_1 . Further cooling below the point P has proceeded with substantially increased cooling rate, changing the transformation start curve as shown in **Figure 6**. Because for the center no incubation time has been consumed, the cooling curve for center starts from temperature A_1 at zero time! In this way the cooling curve for center, which doesn't intersect any pearlitic region, results in higher hardness than the cooling curve for the surface which has started from the point P and intersected a portion of pearlitic region. This is the theoretical explanation of 'inverse' hardness distribution.

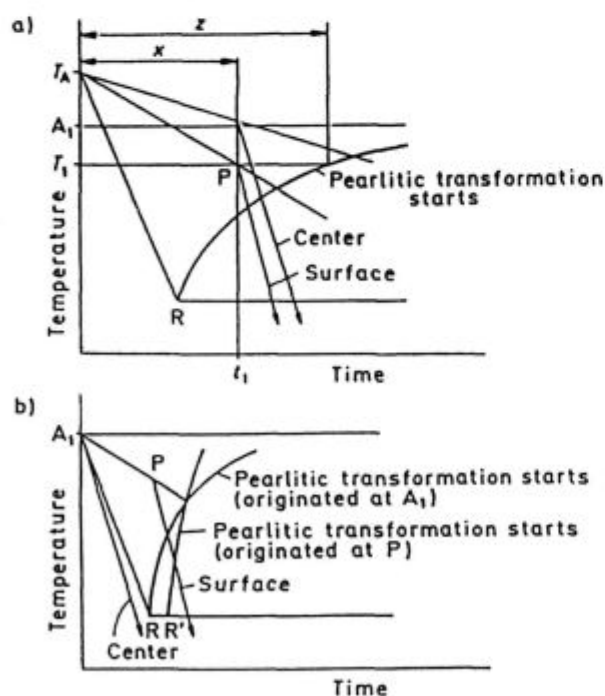


Figure 6: Schematic illustration how delayed quenching causes inverse hardening, according to²

Slika 6: Shematična predstavitev kako kaljenje z zadržanjem ustvari inverzno utrditev. Po viru²

4 HARDNESS DISTRIBUTION AFTER QUENCHING AND AFTER TEMPERING

Figure 7 shows the normal hardness distribution measured across the section of a 50 mm dia bar of AISI-4140 after quenching in ordinary mineral oil of 20°C bath temperature without agitation (curve No 1), and the inverse hardness distribution measured after quenching the same bar in the PAG polymer solution (UCON-E) of 25% concentration, 40°C bath temperature, and 0.8 m/s agitation rate (curve No 2). This shows the high capacity of delayed quenching technique to influence the depth of hardening.

Because low-alloyed structural steels (like the AISI-4140) are used in hardened and tempered condition, it is of interest to see how a normal and an inverse hardness distribution curve, respectively, look like after tempering. **Figure 8** shows this for specimens used to plot the hardness distribution curves in **Figure 7**, after tempering at 480°C for 2 hours. Normal hardness distribution (curve No 1) has retained the same shape as after quenching, while the inverse hardness distribution (curve No 2) gave a uniformly distributed hardness over the cross section. This is result of the known fact that *at tempering the higher hardness values decrease more than the lower hardness values*. The hardness difference at the center of about 6 HRC indicates that inverse hardness distribution guaranties after tempering a structure of tempered martensite in the core, while in case of normal hardness distribution, besides tempered martensite other (softer) structure constituents are present in the core. With regard to mechanical properties, as it is well known (especially for high strength levels), that tempered fine-grained martensite yields the highest toughness of all microstructures.

5 INFLUENCE OF HARDNESS DISTRIBUTION ON FATIGUE PROPERTIES

For bending fatigue tests⁹ especially designed specimens of 300 mm length with the critical diameter of 50 mm were machined of the same heat of the American made steel AISI-4140. All specimens were austenitized in a protective atmosphere to 860°C for 80 minutes. The specimens having normal hardness distribution were quenched one by one, vertically, in used mineral oil of 20°C without agitation. The specimens having inverse hardness distribution were quenched in PAG polymer-solution (UCON-E) of 25% concentration, 40°C bath temperature and 0.8 m/s agitation rate. After quenching all specimens have been tempered in a vacuum furnace at 500°C for 2 hours.

Figure 9 shows the used test rig for bending fatigue tests. All tests were performed in normal environmental conditions under a specific load programme. One round of the used load programme consisted of 7,000 cycles which were subdivided into two parts:

- 5,000 load cycles with the regular load amplitude

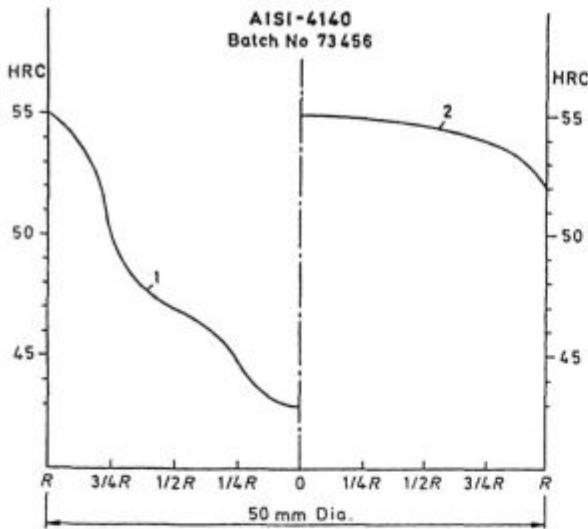


Figure 7: Hardness distribution curves measured on the cross-section of a 50 mm Dia x 200 mm cylinder made of AISI-4140, after quenching under the following conditions:

- 1) Mineral oil of 20°C, without agitation
- 2) PAG polymer-solution (UCON-E) of 25% concentration; 40°C bath temperature and 0.8 m/s agitation rate

Slika 7: Porazdelitev trdote po preseku preizkušanca $\phi 50 \times 200$ mm iz jekla AISI-4140 po kaljenju v naslednjih pogojih:

- 1) mineralno olje, 20°C, brez mešanja
- 2) PAG polimerna raztopina (UCON-E), 25%, 40°C in hitrost mešanja 0.8 m/s

- 2,000 load marker cycles with 25% higher than the regular load amplitude.

The 2,000 load marker cycles were used to obtain information about the crack growth rate and a possible influence of the hardness distribution on it. The information about the crack growth rate is expressed in form of share of the crack growth phase in the total test life:

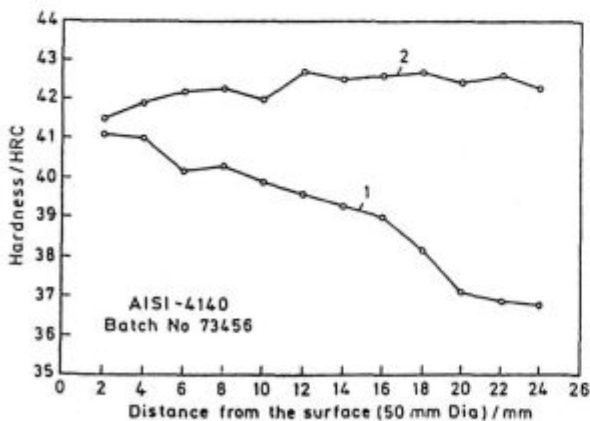


Figure 8: Hardness distribution after tempering at 480°C for 2 hours: 1) Specimen of 50 mm Dia x 200 mm, quenched in mineral oil of 20°C, without agitation

- 2) Specimen of 50 mm Dia x 200 mm, quenched in UCON-E; 25%; 40°C; 0.8 m/s

Slika 8: Porazdelitev trdote po popuščanju 2 uri pri 480°C:

- 1) Preizkušalec $\phi 50 \times 200$ mm kaljen v mineralnem olju pri 20°C brez mešanja
- 2) Preizkušalec $\phi 50 \times 200$ mm kaljen v UCON-E 25%, 40°C, 0.8 m/s

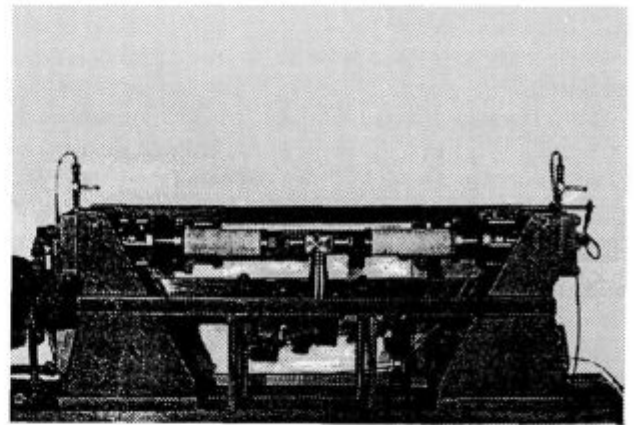


Figure 9: Test rig for bending fatigue tests

Slika 9: Priprava za preizkus upogibne utrujenosti

$$\frac{N_f - N_c}{N_f}$$

in %, where N_f is the number of cycles of the total test life and N_c is the number of cycles to the initial crack. During the tests the cylinder displacement and the load amplitude were recorded to determine N_c and N_f values. The N_c value refers to the beginning of the stiffness loss of the specimen due to initiated crack.

The fatigue tests were performed on different loading levels under pulsating sinusoidal loads with the frequency of $f = 16$ Hz and a stress ratio $R = F_{min}/F_{max} = 0$ which led to the nominal stress amplitudes in the critical area of the specimens. The test results represented by fatigue life to the initial crack versus the nominal stress amplitude (S - N curves) are shown in Figure 10.

Summarising these results it can be concluded, (although the number of tested specimens was low for a statistically confirmed data), that an increased fatigue life was achieved with specimens having inverse hardness distribution compared to specimens having normal

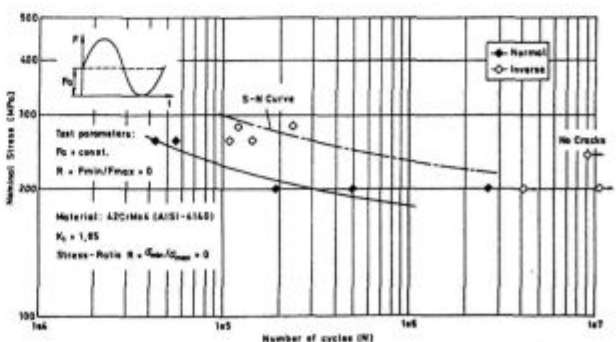


Figure 10: Bending fatigue test results of specimens with normal and with 'inverse' hardness distribution after quenching (both tempered to 500°C for 2 hours)

Slika 10: Rezultati preizkusov upogibne utrujenosti preizkušancev z normalno in z inverzno porazdelitvijo trdote po kaljenju (oba sta bila popuščena 2 uri pri 500°C)

hardness distribution. At the stress level of 270 MPa, at which most tests have been performed, this increase is expressed by a factor of about 7. The crack propagation phase, compared to the total fatigue life was more uniform for specimens with inverse hardness distribution and amounted to 13 to 20%, depending on the stress level. Additional fatigue tests are planned to increase the statistical validity of the achieved results.

6 CONCLUSION

The above described investigation shows that the hardness distribution on the cross-section of the workpiece after quenching can be influenced and greater depth of hardening and better mechanical properties can be achieved by a predetermined and controllable heat transfer dynamics. In future, therefore, the quenching technology will most probably adopt the *control of heat transfer* from the surface of the workpiece instead of letting it occur by itself (depending only on the quenchant and quenching parameters selected), as in today's practice. If so, the question will arise: By which means a controlled heat transfer at quenching is possible?

For liquid, evaporable quenchants (as the hitherto investigations show), this is possible by using polyalkylene-glycol (PAG) polymer-solutions of sufficiently high concentration of adequate temperature and agitation rate. In gas quenching applications (especially in vacuum furnaces with pressurized high velocity gases), more time is available during quenching than in case of liquid quenchants, to change the main cooling parameters i.e. the gas pressure and gas velocity.

In order to find out whether in a particular case the workpiece's cross-section size and hardenability of the steel grade in question are suitable for *quenching with controlled heat extraction dynamics* and to optimize the relevant quenching parameters the computer simulation will be necessary.

The base for such a simulation are the two following requirements:

- The CCT-diagram of the steel-grade in question, which characterizes its hardenability and allows to

overlay the calculated cooling curves for different points on the cross-section, to evaluate the transformation kinetics.

- Heat transfer coefficient values $\alpha = f(t)$ (W/m^2K) between the workpiece surface and the quenching medium for the whole quenching process, characterizing the changes in quenching intensity, which allows to calculate the relevant cooling curves in every cross-section point of different bar diameters.

To get relevant heat transfer data, a workshop designed method to measure and record the quenching intensity of different quenchants, as described in⁸, is required.

7 REFERENCES

- ¹ E. A. Loria: Transformation Behavior on Air Cooling Steel in A3-A1 Temperature Range, *Metals Technology*, (1977) october, 490-492
- ² N. Shimizu and I. Tamura: Effect of Discontinuous Change in Cooling Rate During Continuous Cooling on Pearlite Transformation Behavior of Steel, *Transactions ISIJ*, 17 (1977) 469-476
- ³ N. Shimizu and I. Tamura: An Examination of the Relation Between Quench-hardening Behavior of Steel and Cooling Curve in Oil, *Transactions ISIJ*, 18 (1978) 445-450
- ⁴ B. Liščić, G. E. Totten: Controllable Delayed Quenching, *Proceedings of the International Heat Treating Conference Equipment and Processes*, April 1994, Schaumburg, Illinois, USA, 253-262
- ⁵ M. Chen and H. Zhou: Numerical Heat Transfer Analysis on the Effect of Enhancing the Thickness of the Hardened Layer by Delayed Quenching, Jinshu Rechuli Xuebao (*Transactions of Metal Heat Treatment*), 14 (1993) 4, 1-6 (in Chinese)
- ⁶ B. Liščić, V. Grubišić and G. E. Totten: Inverse Hardness Distribution and its Influence on Mechanical Properties, *Proceedings of the 2nd International Conference on Quenching and the Control of Distortion*, 4-7 November 1996, Cleveland, Ohio, 47-54
- ⁷ B. Liščić: Investigation of the Correlation Between Polymer-Solution (PAG) Concentration and Inverse Hardening Distribution Curves, *Internal Report No 11/92 of Laboratory for Heat Treatment*, Faculty of Mech. Engineering and Naval Architecture, Zagreb, March 1992
- ⁸ B. Liščić, S. Švaić and T. Filetin: Workshop Designed System for Quenching Intensity Evaluation and Calculation of Heat Transfer Data, *Proceedings of the 1st International Conference on Quenching and Control of Distortion*, 22-25 Sept. 1992, Lincolnshire, Illinois, 17-26
- ⁹ *Test Report Nr 7710*, 24 Nov 1994 from the Fraunhofer Institut für Betriebsfestigkeit, Darmstadt, Germany